

### Central European Journal of Chemistry

# Preparation and characterization of high specific surface area $Mn_3O_4$ from electrolytic manganese residue

Research Article

Tiefeng Peng\*, Longjun Xu, Hongchong Chen

Department of Resources and Environmental Science, Key Laboratory for the Exploitation of Southwest Resources and Environmental Disaster Control Engineering of Ministry of Education, Chongqing University, 400044. P.R. China

#### Received 21 January 2010; Accepted 6 May 2010

Abstract: Mn<sub>3</sub>O<sub>4</sub> powders have been produced from Electrolytic Manganese Residue (EMR). After leaching of EMR in sulfuric acid, MnSO<sub>4</sub> solution containing various ions was obtained. Purifying the solution obtained and then adding aqueous alkali to the purified MnSO<sub>4</sub> solution, Mn(OH)<sub>2</sub> was prepared. Two methods were employed to produce Mn<sub>3</sub>O<sub>4</sub>. One way was oxidation of Mn(OH)<sub>2</sub> in aqueous phase under atmosphere pressure to obtain Mn<sub>3</sub>O<sub>4</sub>. The other way was roasting Mn(OH)<sub>2</sub> precursors in the range of 500°C to 700°C. The prepared samples were investigated by using several techniques including X-ray powder diffraction (XRD), Fourier Transformation Infra-Red (FTIR) spectra, and Brunauer-Emmett-Teller (BET) specific surface area instrument. Particle distribution and magnetic measurements were carried out on laser particle size analyzer, vibrating sample magnetometer (VSM). Through XRD, FTIR and determination of total Mn content (TMC), the products prepared were confirmed to be a single phase Mn<sub>3</sub>O<sub>4</sub>. BET specific surface areas can reach to 32 m<sup>2</sup> g<sup>-1</sup>. The results indicated that products synthesized by aqueous solution oxidation method had higher specific surface areas and smaller particle size than those prepared by means of roasting. However the products prepared using the above two methods showed no obvious differences in magnetic property.

Keywords: Waste slag • Mn • Leaching • Roasting • Oxidation

© Versita Sp. z o.o.

### 1. Introduction

 ${\rm Mn_3O_4}$  is used as raw material in the preparation of soft magnetic materials such as manganese zinc ferrite.  ${\rm Mn_3O_4}$  is known to be an effective and inexpensive catalyst to limit the emission of  ${\rm NO_x}$  and CO, which provides a powerful method for controlling air pollution [1,2]. It can be used as a catalyst for oxidation of methane, selective reduction of nitrobenzene [3,4], ion-exchange and molecular adsorption [5,6]. Moreover, catalytic applications of different polymorphs of  ${\rm Mn_3O_4}$  have been extended to combustion of organic compounds at temperatures of 373–773 K. It can also be used as a precursor in the synthesis Li–Mn–O electrode materials for rechargeable lithium batteries [7,8]. It has been shown to be a corrosion-inhibiting pigment [9-11].  ${\rm Mn_3O_4}$  powders with notable increased surface area

and greatly reduced size are expected to display better performance in all the above mentioned applications.

As for methods of Mn<sub>3</sub>O<sub>4</sub> synthesis, generally speaking, when heated to about 1000°C in air [12], all oxides, hydroxides, carbonates, nitrates, and sulfates of manganese can form Mn<sub>3</sub>O<sub>4</sub>. The thermal decomposition approach requires a relatively high reaction temperature, and the products have low specific surface area. The conventional high-temperature calcination preparation of Mn<sub>3</sub>O<sub>4</sub> leads to inconsistency in product quality and is uneconomical. Synthetic techniques based on wet chemistry have been developed for the preparation of Mn<sub>3</sub>O<sub>4</sub> nanocrystals, for example, sol–gel processes, hydrothermal solvothermal methods [13-16]. The sol–gel technique is expensive, time consuming, and polluting. Microwave irradiation method [17], reflux method [18,19], metal organic chemical vapor deposition

<sup>\*</sup> E-mail: ptf1242@yahoo.com.cn

(MOCVD) [20], sol-gel process with KMnO<sub>4</sub> and fumaric acid at high temperature, and sonochemical reaction of Mn(CH<sub>3</sub>COO)<sub>2</sub> with NaOH or etramethylammonium hydroxide (TMAH) [21], surfactant-assisted methods [22] have also been reported. While these methods have provided nanomaterials for fundamental studies, they are obviously not suitable for industrial applications.

EMR are the discarded slag during the production of Electrolytic Manganese. Tons of EMR are discarded every year. In fact, Manganese sulfate could be produced from EMR by leaching. However, it is not easy to remove some impurities such as K and Na, and another disadvantage is that Manganese sulfate is cheap. So it is not economic to produce Manganese Sulfate. It is reasonable to produce  $\mathrm{Mn_3O_4}$ , and the merit to prepare  $\mathrm{Mn_3O_4}$  is that it needs no electric power that is used in the production of Electrolytic Manganese. China's  $\mathrm{Mn_3O_4}$  production scale and output rank first in the world. The production process for  $\mathrm{Mn_3O_4}$  using pricey electrolytic manganese as a raw material makes the production cost high, and products' specific surface areas are low.

The aim of this work was to recover and reuse the slag EMR and to prepare  $\mathrm{Mn_3O_4}$ . In this study, two major methods for synthesis of  $\mathrm{Mn_3O_4}$  were followed. The aqueous solution oxidation method is a simple and promising method for industrial use. The roasting method is seldom employed. Moreover, the reaction mechanism was also investigated. It is a non-hazardous, cost -effective to use EMR as a raw material.

### 2. Experimental Procedure

### 2.1 Materials

EMR were dropped slag from the first pressure filtration or the second pressure filtration, or the mixture of the two.

Fresh EMR with high moisture content was obtained from Xiushan, Chongqing in Nov. 2008, air dried in hot sun, well mixed, and then ground to -120 mesh small particles. The chemical compositions are listed in Table 1.

XRD, chemical analysis showed that the main minerals in the slag are quartz, gypsum, mullite and hematite.

Table 1. The chemical compositions of EMR

Mn	SiO <sub>2</sub>	Fe	Al	Р
3.6%	42.3%	2.81%	2%	0.24%

### 2.2 Preparation of Mn<sub>3</sub>O<sub>4</sub>

### 2.2.1 Leaching of EMR in sulfuric acid and purifying the produced solution

Leaching experiments were done under the conditions of solid to liquid ratio 1:3 (g g<sup>-1</sup>), 20%  $\rm H_2SO_4$  (g g<sup>-1</sup>) for 4 h at 90°C.

The leached solution was filtered twice, and then added an appropriate amount of  $3\% \ H_2O_2$  as oxidant to turn  $Fe^{2+}$  to  $Fe^{3+}$  at  $60^{\circ}C$ . After the oxidation reaction was complete, sodium hydroxide was added to the solution to adjust pH to 5.4, and observed for 1 h.  $Al(OH)_3$  and  $Fe(OH)_3$  could form precipitates,  $Al^{3+}$ ,  $Fe^{3+}$  were removed by filtering. BaS was added to the solution to remove heavy metal ions.  $Mg^{2+}$  and  $Ca^{2+}$  can be removed by adding an appropriate amount of NaF.

The purification technology is well-developed and is similar to the purification in the process of preparation of electrolytic manganese. However attention should be paid to the dose of purifying agent.  $MnSO_4$  solution, which contained small amounts of  $K^+$ ,  $Na^+$ , was prepared after the ions of Fe, Al, Ca, Mg, heavy metal ions were removed.

### 2.2.2 Preparation of Mn(OH), by precipitation

The reaction formula of Mn(OH)<sub>2</sub> preparation was as follows:

$$MnSO_4 + 2OH^- = Mn(OH)_2 + SO_4^{-2}$$

 ${\rm Mn(OH)}_2$  was produced by adding dilute aqueous ammonia to purified  ${\rm MnSO}_4$  solution at room temperature. And then, the reacted solution was statically kept for 2 h without moving in order to form  ${\rm Mn(OH)}_2$  precipitates. Orange/brown  ${\rm Mn(OH)}_2$  was precipitated and separated via filtration by suction pump.

The  $\mathrm{Mn(OH)}_2$  precipitates were washed with distilled water several times until  $\mathrm{SO_4}^{2}$  was not detected.  $\mathrm{BaCl}_2$  solution was added to filtered water to detect  $\mathrm{SO_4}^{2}$ . It indicated the  $\mathrm{SO_4}^{2}$  was non-existent if there was no precipitate.

The Na $^+$ , K $^+$  and other soluble ions had been removed after  $\mathrm{Mn(OH)}_2$  precipitates were fully washed, and will not affect the final product quality.

The above precipitates were separated to several parts. Some were used for 2.2.3. The others were dried at 100°C overnight to get Mn(OH)<sub>2</sub> precursors for 2.2.4.

## 2.2.3 Synthesis by oxidation of Mn(OH)<sub>2</sub> in aqueous phase

The following tests and procedures were employed for preparing  $\rm Mn_3O_4$  in aqueous medium.  $\rm Mn_3O_4$  was obtained by oxidation of  $\rm Mn(OH)_2$  in aqueous phase under atmosphere pressure. The  $\rm Mn(OH)_2$  was obtained

from step 2.2.2. Aqueous turbid liquid of  $Mn(OH)_2$  was obtained by adding an appropriate proportion distilled water to  $Mn(OH)_2$ . The samples produced were indexed with nomenclature using short names as shown in Table 2.

Blank tests: The turbid liquid of  $Mn(OH)_2$  was oxidized by pump air at 80°C for 4 h. No chemical reagents were added during the oxidation process. The reactive products  $(Mn_2O_4)$  were dried at 100°C.

Hydrazine hydrate tests: Adding hydrazine hydrate to reaction system during the process of oxidation, other processes were the same as the blank test.

Ethanol tests: (1) Reaction condition was the same as blank test. The ethanol was added to dried process of precipitates ( $Mn_3O_4$ ) at 100°C. (2) Ethanol was added to the reaction system, and in  $Mn_3O_4$  dry process at 100°C. The other processes were the same as the blank test.

 $\rm H_2O_2$  tests: not pump air to the mixed aqueous media, using  $\rm H_2O_2$  as an oxidant. The other processes were the same as the blank group.

 $\mathrm{NH_4OH}$ - $\mathrm{NH_4Cl}$  buffer solutions tests (20 g Ammonium Chloride, 100 mL 28% ammonia 100 mL, in 1000 mL solution, pH=10): The 20 mL or 40 mL of  $\mathrm{NH_4OH}$ - $\mathrm{NH_4Cl}$  buffer solution was added in the turbid liquid of washed  $\mathrm{Mn(OH)}_2$  (each containing 0.02 mol Mn) and other processes were the same as the blank group.

The above methods are all indexed in Table 2.

A surfactant or ethanol was added to the reaction medium to prevent the agglomeration. If using other surfactants, the quality of produced  $\mathrm{Mn_3O_4}$  cannot be guaranteed because it is hard to remove the impurities brought by surfactants. Ethanol is easy to eliminate, which has no bad effect on the produced  $\mathrm{Mn_3O_4}$ 's quality and TMC (total manganese content).

It had also been confirmed in the following results that TMC of the samples prepared by adding ethanol could meet the requirement of first class quality.

Hydrazine hydrate was used to control potential fluctuation during oxidation process in the medium.

### 2.2.4 Synthesis of $Mn_3O_4$ by roasting $Mn(OH)_2$ precursors

The produced  $\mathrm{Mn(OH)_2}$  precursors were from 2.2.2, adding a small amount of ethanol to the produced  $\mathrm{Mn(OH)_2}$  precursors and mixing, then drying the mixed medium at 100°C. The dried precursors were put into a muffle furnace for heating at 500°C -700°C for 1.5 h and the brown  $\mathrm{Mn_3O_4}$  powders were obtained.

#### 2.3 Measurements

Determination of manganese content in EMR was referred to GB 1506-2002, ammonium iron (Fe<sup>2+</sup>) sulphate titrimetric method, oxidized by perchloric acid.

EDTA method (HG/T 2835-1997) was chosen to determine the TMC of the produced samples.

The above 2 analysis methods were performed according to national standards in China.

XRD analysis was conducted on a Shimadzu XRD 6000 using Cu Kα operated at 40 KV, 30 mA. Scan range was from 10° to 80°, scan mode was Continuous Scan, and scan speed was 2.0000 (deg min<sup>-1</sup>).

Fourier Transformation Infra-Red (FTIR) spectra were taken on Nicolet (5DX-550II). Samples for characterization were prepared by mixing with KBr, and scan range was from 4000 to 400 cm<sup>-1</sup>.

Magnetic measurements were carried out with the Lake Shore VSM-7407 to obtain M-H curves.

BET surface areas measurement was performed on Micromeritics ASAP 2010. The samples were treated at 100°C, to expel gas and water in sample. The specific surface area of the samples was determined by the BET method. The pore size and distribution were extrapolated using the BJH desorption data.

Particle distribution was carried out on laser particle size analyzer (Rise-2008). No surfactant was used during the test.

### 3. Results and Discussion

# 3.1 Results of TMC in produced $Mn_3O_4$ samples

TMC of Mn<sub>3</sub>O<sub>4</sub> is 72.03% in theory.

### 3.1.1 Samples Synthesized by oxidation of Mn(OH)<sub>2</sub> in aqueous phase

The results are presented in Table 2, A. symbolized for Aqueous solution oxidation method.

Through these experiments that involved the use of H<sub>2</sub>O<sub>2</sub> as an oxidant and from the results of TMC of the samples produced, it is evident that H2O2 is not a good oxidant for producing Mn<sub>3</sub>O<sub>4</sub>. It is not easy to control the degree of oxidation reaction. And it is difficult to choose an appropriate amount of H2O2, for dosage since it has a very critical influence on the final samples produced. MnO<sub>2</sub> may easily be formed by oxidation of Mn(OH)<sub>2</sub> using H2O2. It can be found from experiments that the color of the mixed solution suddenly turns to black by adding a medium concentration of H2O2 indicating the formation of MnO<sub>2</sub>. So, the concentration of H<sub>2</sub>O<sub>2</sub> should be very dilute and the rate of addition should be slow, otherwise one cannot get uniform or a single phase Mn<sub>3</sub>O<sub>4</sub>. Mn(OH)<sub>3</sub> could easily be overly oxidized to MnO<sub>3</sub> if H<sub>2</sub>O<sub>2</sub> is used as an oxidant. For example,

 $3Mn(OH)_{2} + H_{2}O_{2} = Mn_{3}O_{4} + 4H_{2}O_{2}$ 

Table 2. The all aqueous solution oxidation method and TMC of samples

Group	Samples	During oxidation process	Adding to dry	TMC
Blank group	A.Blank	pump air	~	69.151%
Hydrazine hydrate group	A.Hh	Pump air+ Hydrazine hydrate	~	71.226%
, , , , ,	A.pe	pump air	ethanol	70.723%
Ethanol group	A.pee	pump air + ethanol	ethanol	72.035%
H <sub>2</sub> O <sub>2</sub> group	A.H <sub>2</sub> O <sub>2</sub>	H <sub>2</sub> O <sub>2</sub>	~	67.988%
2 2	A.B40	pump air+40 mL	~	71.495%
Buffer solutions group	A.B20	pump air+20 mL	~	71.495%

From the formula above, 1 mol  $Mn(OH)_2$  need 1/3 mol  $H_2O_2$ , however in the experiment  $Mn(OH)_2$  could be overly oxidized to  $MnO_2$  even though less than 1/3 mol  $H_2O_2$  was added.

From the results above, we find that TMC (69.15%) of Blank test (Sample A.Blank) is relatively low compared with samples using other methods. Adding ethanol to dry at 100°C (Sample A.pe) showed little increase in the final TMC (70.723%); From Sample A.pee (72.035%), we find that adding ethanol during oxidation to the mixed medium resulted in a marked increase of the final TMC. Addition of ethanol is useful for intensifying exposure  $\mathrm{Mn}(\mathrm{OH})_2$  with  $\mathrm{O}_2$  due to its high volatility. Ethanol is also useful due to its surfactant function, which is good for the process.

Adding hydrazine hydrate during oxidation (Sample A.Hh) has a significant effect on the final TMC (71.226%), and TMC of the produced  ${\rm Mn_3O_4}$  could satisfy the criteria of the best product.

From Sample A.B40 and Sample A.B20, we find that adding  $\mathrm{NH_4OH\text{-}NH_4Cl}$  buffer solutions contributes to a large increase in the final TMC. However the dosage of buffer solutions added was not very important for the final TMC. Buffer solutions could keep stability of pH in the mixed medium. Without Buffer solutions, acidity of some region in the mixed medium may be too high, while other parts may be too low, which may result in impurities such as  $\mathrm{Mn_2O_3}$  and  $\mathrm{MnOH}$  in the oxidation process.  $\mathrm{NH_4OH\text{-}NH_4Cl}$  buffer solutions could prevent grain aggregation due to its catalysis effect. Its catalysis effect possibly affects particle collision by allowing colloidal  $\mathrm{Mn(OH)_2}$  to detach from the surface of the reaction, so the reaction could be continued.

### 3.1.2 Samples prepared by roasting Mn(OH)<sub>2</sub> precursors in the range of 500°C to 700°C.

The produced  $\mathrm{Mn(OH)}_2$  precursors which come from 2.2.2 were dried. The results are presented in Table 3. Samples B.9 to B.13 are indexed in the table.

From the results, TMC of all samples produced are relatively low and do not reach the standard of the average quality. In the range of 500°C to 700°C, roasting temperature made no obvious effect on the final samples'

 Table 3. TMC of samples by roasting

B.9	700°C	70.787%
B.10	650°C	69.986%
B.11	600°C	69.986%
B.12	550°C	70.416%
B.13	500°C	69.675%

TMC. At 700°C, TMC increased a lot. Combining TMC and XRD studies below, we could find that producing by roasting method for 1.5 h is not a good method, because the samples produced contained impurities such as  $\rm Mn_2O_3$ . Namely, it is hard to obtain a single phase  $\rm Mn_3O_4$  by roasting method.

### 3.2 XRD analysis

PDF#24-0734: Cell=5.7621 Å × 9.4696 Å

 $\rm Mn_3O_4$  has two crystal structures: below 1433 K  $\rm Mn_3O_4$  exhibits tetragonal structure as  $\rm Mn^{2+}[Mn^{3+}]_2O_4$ ; above 1433 K  $\rm Mn_3O_4$  exhibits cubic structure as  $\rm Mn^{2+}[Mn^{2+}Mn^{4+}]O_4$ 

Using software JADE 5.0 to analysis the XRD data of the produced samples, crystal grain size and the lattice constants could be obtained.

The crystal grain size can also be evaluated using the Scherrer formula,  $d = k\lambda/(\beta cos\theta)$ , Where  $\lambda$  is the X-ray wavelength,  $\theta$  is the Bragg angle and  $\beta$  is the halfpeak width in radians.

The XRD patterns of samples were in Fig.1.

Results were as follows:

For sample A.pee: Refined Cell = 5.7605, 9.45027; Size is 31 nm

For sample A.B40: Refined Cell = 5.76223, 9.45422; Size is 29 nm

For sample B.12: Refined Cell = 5.75732, 9.45316; Size is 60 nm-67 nm

For sample A.pee, a=b $\neq$ c. It indicates that sample produced has tetragonal structure. All diffraction peaks can be perfectly indexed to the hausmannite structure (JCPDS Card 24-0734). The lattice constants were consistent with those of bulk  $Mn_3O_4$  (PDF File No. 24-734). No peak, which is corresponding to impurity phases such as other forms of manganese oxides MnO and  $Mn_2O_3$ , were detected.

For sample A.B40, was similar with sample A.pee.

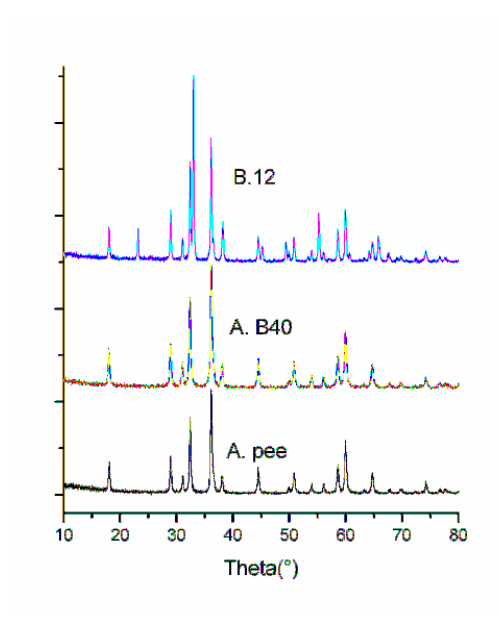


Figure 1. The XRD patterns of samples A.pee, A.B40, B.12

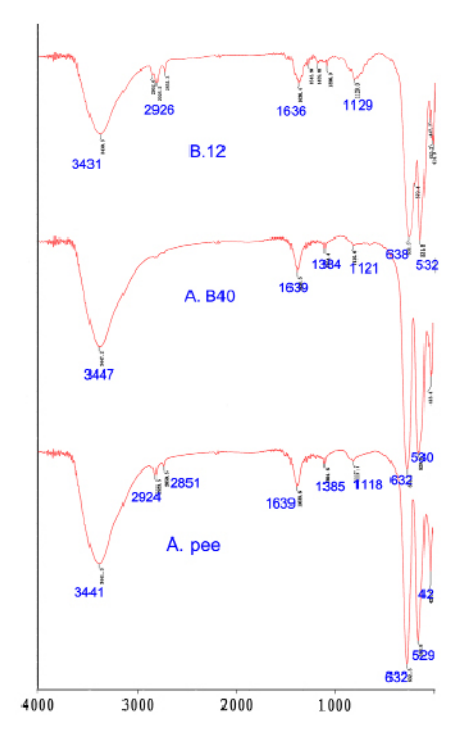


Figure 2. FTIR spectroscopy patterns of A.pee, A.B40, B.12

For sample B.12, according to XRD result, hausmannite ( $Mn_3O_4$ ) and manganese oxide ( $Mn_2O_3$ ) were detected. It indicates that sample produced by roasting at 550°C contained small amounts of manganese oxide ( $Mn_2O_3$ ), which was mentioned in Part 3.1.2. Please note, it could be distinguished between hausmannite ( $Mn_3O_4$ ) (JCPDS card No.24-0734) and  $Mn_2O_3$  (cubic  $Mn_2O_3$ : JCPDS card No.65-7467;

Orthorhombic  $\rm Mn_2O_3$ : JCPDS card No.24-0508) due to the intensity of some diffraction peaks (20# 32.9, 23.1, 55.1) which can enable the distinction. JCPDS card No.65-7467 is greatly similar to JCPDS card No.24-0508.

The size evaluated using Scherrer formula was primary or original particle. However the size data tested by particle size analyzer reflected average size of the agglomerated particle. The particle size analyzer test was conducted in aqueous medium. The two test methods are based on different theories, so the test conditions were different.

Therefore it was not strange to observe large differences between the data evaluated by the two methods. The size tested by particle size analyzer was about 1  $\mu$ m, which was significantly larger than 60 nm; the reason was that Mn<sub>3</sub>O<sub>4</sub> particle became agglomerateed through hydration during the test process in aqueous medium; the agglomerated size could be called as the second particle compared to primary particle. In fact, the size usually could reach nm degree, and often below 100 nm when using Scherrer formula to evaluate size.

Comparing sample B.12 with A.pee, A.B40, the XRD peaks in B.12 were sharper than that of A.pee and A.B40. This suggests that sample B.12 had a better crystal structure. Therefore, the fine and sharp peaks in B.12 indicated its better crystal growth, which was also the microcosmic exhibition of larger grain size. But bigger grain size was not good for the quality of the products. So, we could find that high temperature roasting could lead to better crystal growth, bigger grain size compared with drying at 100°C in aqueous solution oxidation method. That is to say that temperature has great effect on grain size.

### 3.3 FTIR spectrum

FTIR spectroscopy patterns are presented in Fig.2.

Vibrational spectra of manganese oxides can be divided into three regions at 750–600, 600–450, and 450–200 cm<sup>-1</sup>, where stretching, bending and wagging vibrations of MnO<sub>2</sub> units are showing up respectively.

Three significant absorption peaks are observed in the range of 400–650 cm<sup>-1</sup> for these three samples; the vibration frequency at 631–638 cm<sup>-1</sup> [632(A.pee), 632(A.B40), 638(B.12)] is characteristic of Mn–Ostretching modes in tetrahedral sites, whereas vibration frequency at 529–532 cm<sup>-1</sup> corresponds to the distortion vibration of Mn–O in an octahedral environment. The third vibration band, which locates at a weaker wave number, 418–425 cm<sup>-1</sup>, can be attributed to the vibration of manganese species (Mn³+) in an octahedral site [23]. The FTIR spectrum was consistent with reported references for Mn₃O₄ [24-26].

Table 4. The BET results of samples by various methods

Samples	BET Surface Area	Langmuir Surface Area	Volume	Pore Size	Cubic Size	Ball Size
A.Hh	21.1781	30.7017	0.12	23	58.6	29
A.pe	21.8018	30.5419	0.10	18	56.9	28
A.pee	28.0077	38.6468	0.18	26	44	22
A.B40	32.3986	44.7475	0.19	22	38.3	19
B.11	13.1590	18.3454	0.04	11	94.1	47

The weak absorptions at 2924-2962 and 2851-2853 (A.pee, B.12) cm<sup>-1</sup> were due to C--H stretching modes, which indicated the existence of trace amount of ethanol in A.pee, B.12. The ethanol could decompose during drying and roasting process.

The very weak peaks at 1384-1387 cm $^{-1}$  and 1118-1130 cm $^{-1}$  in all the three samples were attributed to S related stretching vibration, which revealed that trace amount of S related materials were bonded to the surface of  $Mn_3O_4$ . The S could become an impurity in final products during drying and roasting process.

For A.pee and A.B40, the X-ray pattern fully coincide with JCPDS 24-0734 for hausmannite, combining FTIR and XRD studies ensure fast and reliable proof of  $\mathrm{Mn_3O_4}$ .

For sample A.B40, no vibration bands relating to the surfactant (vibration bands of  $-\mathrm{CH}_2$ ,  $-\mathrm{CH}_3$ ,  $-\mathrm{NH_4}^+$ , etc) are detected. It indicated that the as-prepared  $\mathrm{Mn_3O_4}$  surface is free of ethanol and  $\mathrm{NH_4CI}$ , which is also consistent with the fact that A.B40 was prepared by not adding ethanol.

Finally, a broad band at 3430-3447 cm<sup>-1</sup> (A.pee: 3441 cm<sup>-1</sup>, A.B40: 3447 cm<sup>-1</sup>, B.12: 3430 cm<sup>-1</sup>)and another weak band at 1636-1639 cm<sup>-1</sup> were observed due to the absorbed water, which were stretching and bending vibrations of water molecules.

#### 3.4 BET surface areas

The results were listed in Table 4. The BET Surface Area and the pore size distribution were calculated by BET and BJH model.

Area: m<sup>2</sup> g<sup>-1</sup>; Volume: cm<sup>3</sup>g<sup>-1</sup>; Size: nm

Cubic Size =  $6/(S^*\rho)$ ; Ball size =  $3/(S^*\rho)$ ; S is BET Surface Area,  $\rho = 4.83$  g cm<sup>-3</sup>

Cubic Size and Ball Size were evaluated by regarding the produced products' shape as cube, ball respectively using the above formula.

Volume - average volume; Pore Size - average pore diameter; Cubic Size, Ball Size - average grain size.

From the above table, sample A.B40, which was prepared by adding NH<sub>4</sub>OH-NH<sub>4</sub>Cl buffer solutions, had largest BET Surface Area. Contrary to sample A.B40, sample B.11 which was prepared by roasting method

had the smallest BET Surface Area.

A.Hh, A.pe, A.pee, A.B40 were all synthesized in aqueous phase. Surface area of product synthesized by oxidation of  $\text{Mn}(\text{OH})_2$  in aqueous phase was larger than that of product of roasting (B.11) [27].  $\text{NH}_4\text{OH-NH}_4\text{Cl}$  buffer solutions had a significant effect on the increase of the products' Surface Area, which could be seen clearly from the above table.

A.Hh was not adding ethanol; A.pe was not adding ethanol throughout the oxidation process but adding ethanol to the precipitates to dry at 100°C; A.pee was produced by adding ethanol throughout the oxidation process.

From samples A.Hh, A.pe, A.pee, we could find that adding ethanol throughout the oxidation process had great influence for the increase of products' surface area; adding ethanol to the precipitates ( $\mathrm{Mn_3O_4}$ ) to dry had little effect for the increase of products' surface area. The reasons that caused the above differences could be explained as follows: roasting at high temperature could damage the micro-structure of the products, so impaired the capacity of adsorption in the final products.  $\mathrm{NH_4OH-NH_4Cl}$  buffer solutions may have catalysis effect, which could build a proper medium for the growth of microstructure.

The Langmuir Surface Area had the same trend as BET Surface Area, which is only different in number.

As for average volume, roasting at high temperature could lead to low average volume (0.04 cm³ g⁻¹). For average pore diameter, roasting could lead to small average pore diameter (11 nm) and big average grain size, which was confirmed by XRD analysis in part 3.2.

Generally, porous materials could be classified to three types: Micro porous, Meso-porous, Macro porous material according to their Pore Size. Micro porous material has average pore diameter smaller than 2 nm, while Macro porous lager than 50 nm; Meso-porous material has average pore diameter between 2 nm-50 nm. So the produced samples were all Meso-porous material. Generally, for particle materials, BET Surface Area is an important character. The materials are Meso-porous, so it is also necessary to study their pore size distribution.

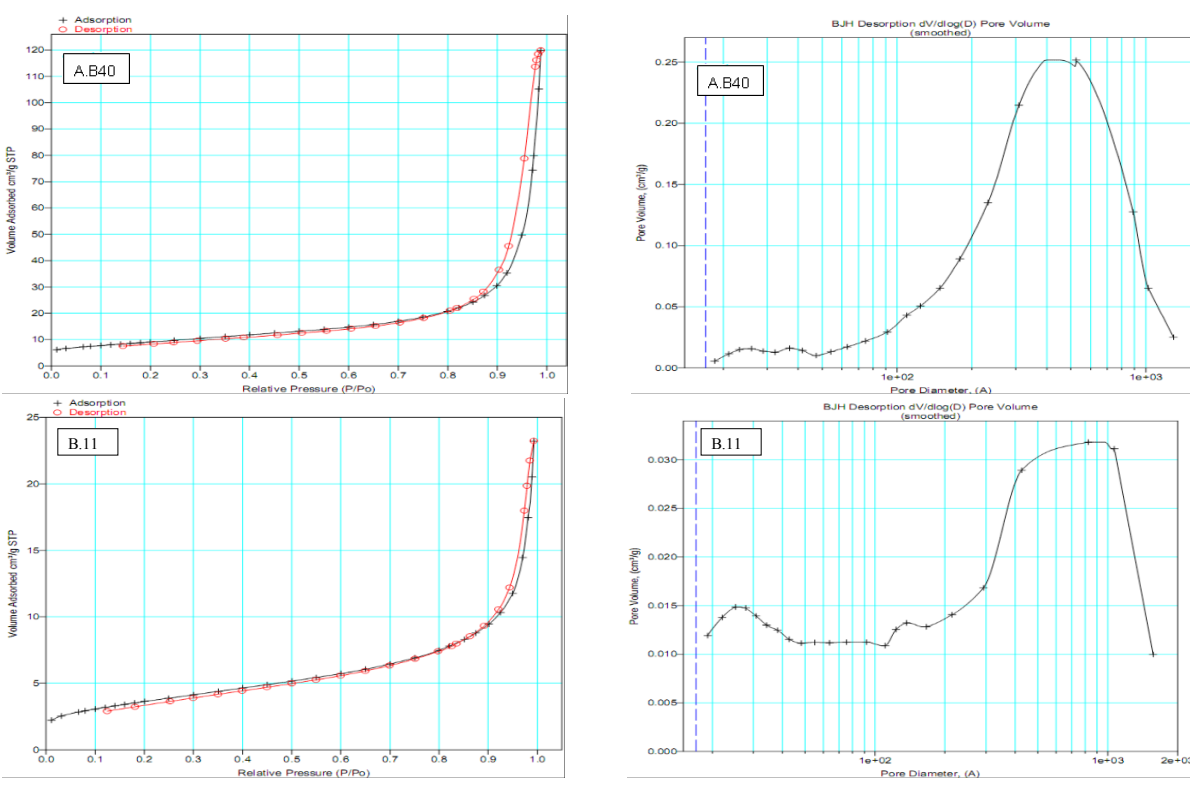


Figure 3. N<sub>2</sub> adsorption-desorption isotherms at 77 K and pore size distribution of the as-prepared Mn<sub>2</sub>O<sub>4</sub> samples, A.B40, B.11

The results of adsorption-desorption isotherms and pore size distribution for A.B40, B.11 were in Fig. 3. Other samples are similar to the two samples.

According to BDDT [28] and IUPAC [29,30] adsorption isotherms system, the samples all showed IV type isotherms, which indicated that the samples could form limited multilayer adsorption.

From the Fig. 3, the  $\rm N_2$  isotherms exhibit a capillary condensation step at p/po $\approx$ 0.85–0.98, which could be indicated by hysteretic loop. This phenomenon usually occurred in Meso-porous adsorption. The hysteretic loop belonged to H3 type according to IUPAC isotherms system, which showed that the adsorption exhibited unlimited adsorption volume at relatively high pressure and the adsorption volume increased with the rising of pressure. This type of hysteretic loop usually occurred in materials which have long, narrow porous structure.

According to BJH desorption pore distribution, the porosity in the samples are made up of pores centered at: 54 nm for A.Hh, 47.4 nm for A.pe, 53.3 nm for A.pee, 52.5 nm and 30.9 nm for A.B40, and 42.7 nm for B.11.

#### 3.5 Particle size distribution

A.pee: 0.67  $\mu$ m; A.B20: 0.73  $\mu$ m; B.12: 17  $\mu$ m Particle size range: A.pee, 0.1  $\mu$ m-3.1  $\mu$ m; A.B20, 0.1-3.1; B.12, 4.9-46.6

Particle size distribution analysis reveals that the

second particle size of the products by preparing in aqueous medium was smaller than that of roasting method.

The results were very different from data evaluated by XRD analysis. However the difference could be explained easily, they used different testing methods which based on different principle.

### 3.6 Magnetic Properties

The results of Magnetic Properties were as below in Fig. 4.

A.pee had the similar M–H curves as B.11.

The results were as follows:

B.11 Coercivity (Hci)=2.6371 G

Magnetization (Ms)= $19.046\times10^{-3}$  emu 0.71 emu g<sup>-1</sup> A.pee Coercivity (Hci)=1.4684 G

Magnetization (Ms)=13.457×10<sup>-3</sup> emu 0.71 emu g<sup>-1</sup>

Generally,  ${\rm Mn_3O_4}$  nano-crystals show an obvious ferromagnetic behavior at low temperatures. The magnetization is hard to reach saturation at room temperature.

M–H curves in Fig. 4 are linear with the field and have no coercivity at room temperature, which could be foreseen that the magnetization never gets saturated even at very high applied field.

The two tested samples were both with no apparent saturation magnetization and hysteresis, which were

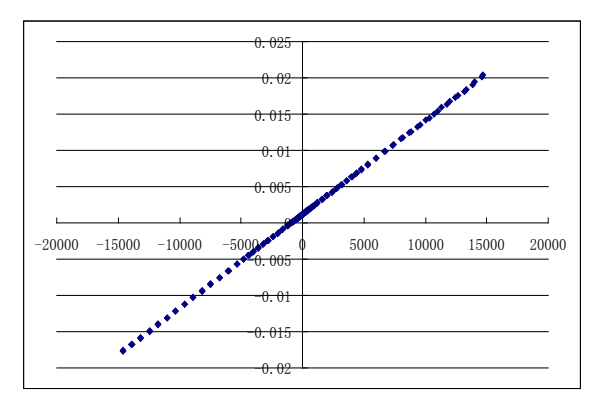


Figure 4. Room temperature M-H curves for Mn<sub>3</sub>O<sub>4</sub> synthesized using roasting method, B.11

consistent with the bulk Mn<sub>3</sub>O<sub>4</sub>.

Room temperature magnetization curves for both samples showed no hysteresis, indicating the super paramagnetic character of the samples. The difference in synthesized methods did not cause difference in their room temperature magnetization behavior.

# 3.7 Effect of synthesis parameters on the final material properties

Generally, synthesis parameters contained temperature, pH, reaction time  $\it etc$ . For aqueous solution oxidation method, the temperature could be about  $80^{\circ}$ C for 4 h during oxidation process. If the temperature was too low, the oxidation reaction rate would be slow. However if the temperature was too high, the grain size of the products would be big, which is not good for the quality of products. The pH of the mixed medium during oxidation process should be in a suitable range, which was discussed in part 3.8.2. The reaction time was about 4 h, if the time is too long, that could be a waste; however if the temperature was low, the reaction time should be longer. As for the magnetic property, as long as the products were  $\rm Mn_3O_4$ , that were no obvious differences.

# 3.8 Reaction mechanism of Mn and oxygen in aqueous solution

### 3.8.1 The difference between industrial production method and the method used by this study

At present,  ${\rm Mn_3O_4}$  powders are mostly produced by electrolytic manganese in China. The production process is as follows: using electrolytic manganese as raw material, the electrolytic manganese is ground to fine particles and put into solution. Ammonium salt as a catalyst is added to the mixed medium. Air is pumped to the medium at a certain temperature.  ${\rm Mn_3O_4}$  is obtained by complete oxidation of  ${\rm Mn.}$  The detailed reaction mechanism is as follows.

Mn +  $(NH_4)_2SO_4$  +  $2H_2O$  = MnSO<sub>4</sub> +  $2NH_4OH$  +  $H_2\uparrow$ Newly produced MnSO<sub>4</sub> could react with  $NH_4OH$ and form intermediate products, namely manganese ammonium complexes,

 $MnSO_4 + xNH_4OH = Mn(NH_3)_xSO_4 + xH_2O$ 

The manganese ammonium complexes produced are unstable and could get converted to  $Mn(OH)_2$ .  $Mn(OH)_2$  would transfer to  $Mn_2O_4$  by pumping air,

 $6Mn(OH)_2 + O_2 = 2Mn_3O_4 + 6H_2O$ 

For the whole process, the reaction could be simplified as,

 $6Mn + 6H_2O + O_2 = 2Mn_3O_4 + 6H_2\uparrow$ 

In the whole process, ammonium sulfate was added as a catalyst. The former half part of the reaction could be regarded as the hydrolysis reaction of Mn. In fact, the latter half part could be recognized as aqueous solution oxidation method.

### 3.8.2 Two stage oxidation method

Two stage oxidation method was as follows: the first step was preparation of  $Mn(OH)_2$ , the second stage was oxidization of  $Mn(OH)_2$  to  $Mn_3O_4$ .

From Fig. 5, the  $\rm H_2O_2/O_2$  line and  $\rm O_2/H_2O$  line are both above  $\rm Mn_3O_4$  region, which indicates that  $\rm H_2O_2$  or  $\rm O_2$  could both oxidize  $\rm Mn(OH)_2$  to  $\rm Mn_3O_4$  theoretically. However, if not controlled properly, the samples produced may be  $\rm MnO_2$ ,  $\rm Mn_2O_3$ , or a mixture of a variety of manganese oxides. According to the above figure, when pH is above 6.5 it is suitable for the formation of  $\rm Mn_2O_4$ .

From the Fig. 5, there are two ways to prepare  $\mathrm{Mn_3O_4}$ . (1) Mn could be first transferred to  $\mathrm{Mn^{2+}}$ , then pH controlled at 6.4-7.6 in aqueous solution and  $\mathrm{Mn^{2+}}$  oxidized by air; (2) Mn could be first transferred to  $\mathrm{Mn(OH)_2}$  precipitate and then oxidized by air.

If the first method is applied then Mn is oxidized in MnSO<sub>4</sub> solution (in other words, in the process of oxidation), there are too many SO<sub>4</sub><sup>2-</sup> in the medium and these impurities (SO<sub>4</sub><sup>2-</sup>) could blend in the final products, which could impair the quality of products. Reaction formula,

$$6Mn^{2+} + O_2 + 6H_2O = 2Mn_3O_4 + 12H^+$$

From the formula, the reaction would also produce H<sup>+</sup>. So in order to keep the medium in a stable pH range, alkali should be added. The process requires a narrow and strict pH range. It's difficult to keep an appropriate pH.

If the second method is adopted, the process will not produce any acid or alkali and there is vast stable space above Mn<sub>3</sub>O<sub>4</sub>, which indicates that the reaction does not need strict pH range.

Comparing the advantages and disadvantages of both ways, we could find that the second method is

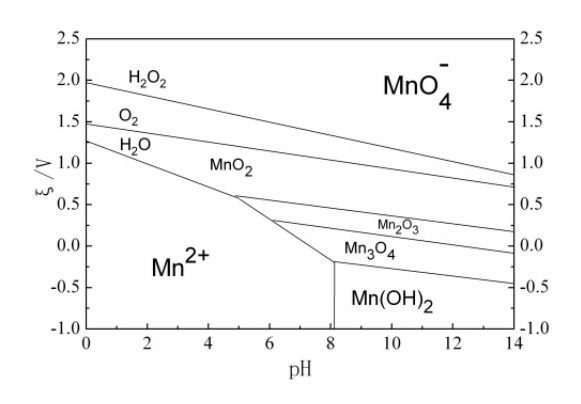


Figure 5. Potential—pH of Mn—O system in aqueous solution at 80°C

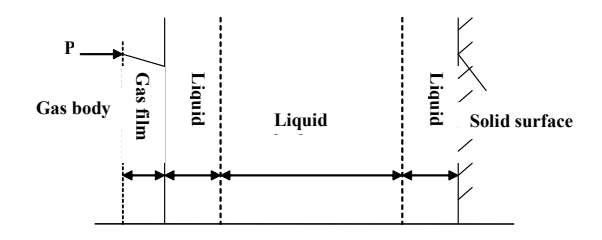


Figure 6. Sketch map for distribution of concentration in gas-liquidsolid reaction

more stable and convenient.

Applying the first method, through the experiment of one-step air oxidation, adding ammonia to regulate pH, the final products' manganese content usually was about 63%-68%. The products were black, proving they had been over-oxidized. So the first method was not suitable for preparing  $\mathrm{Mn_3O_4}$ .

To improve the recovery ratio of manganese, the amount of ammonia added could be a little more in the process of preparing  $Mn(OH)_2$ .

However, too high concentration of  $\mathrm{NH_4}^+$  in the medium will lead to partly dissolution of  $\mathrm{Mn(OH)_2}$  and decrease the recovery ratio of manganese.

Adding ammonium persulfate as an oxidant, the result showed that it was difficult to control the extent of oxidation due to its strong oxidation character. The crystal structure of products was damaged seriously and impurity content of the products was too high. So ammonium persulfate was not a good oxidant for preparing  $\mathrm{Mn}_3\mathrm{O}_4$ .

### 3.8.3 Analysis of Mn(OH), oxidation process

It was a gas-liquid-solid reaction that Mn(OH)<sub>2</sub> was oxidized to Mn<sub>3</sub>O<sub>4</sub> by air in aqueous medium. The

reaction occurred on the surface of solid. According to the double-membrane theory, the whole process included the following steps,

- 1) Oxygen of gas-phase diffused in gas-liquid interface through gas-film.
- 2) Oxygen dissolved in the gas-liquid interface, through the interface into the liquid film, and then spread to the liquid phase within the main liquid body.
- 3) Oxygen in the liquid phase with a uniform concentration will further spread to the solid particles through liquid-film, and the liquid-film was at the surface of solid.
- Oxygen and liquid-phase components reacted on the solid surface.

The whole reaction process occurred orderly according to the above steps. Combining with double-membrane theory, the sketch map of gas-liquid-solid reaction was as below in Fig. 6.

### 4. Conclusions

A variety of methods were employed to prepare Mn<sub>3</sub>O<sub>4</sub> using EMR as a material, the products were investigated by TMC and characterized by XRD, FTIR, BET, etc. The methods could be divided into two main types, aqueous solution oxidation method and roasting method. The products using aqueous solution oxidation method were of better quality than those made using roasting method. For instance, they had better chemical composition, better BET surface areas property, and smaller particle diameter. They showed no obvious difference in Magnetic Property. For the aqueous solution oxidation method, adding NH<sub>2</sub>OH-NH<sub>2</sub>Cl buffer solutions (pH=10) had a good effect on final products' chemical composition and BET surface areas. Using H<sub>2</sub>O<sub>2</sub> as an oxidant could lead to over-oxidation, so it is not a good method to prepare  $Mn_3O_4$  by using  $H_2O_2$  for oxidation of  $Mn(OH)_2$ . Finally, reaction mechanism of Mn and oxygen in aqueous solution was studied, which could explain the difference between industrial production method and the method used by aqueous solution oxidation method, and could also explain the reason why choose this method.

### **Acknowledgements**

This project was financially supported by the Chongqing Science and Technology Commission (CSTC, 2010AC4054).

#### References

- [1] M. Baldi, F. Milella, G. Ramis, V. Sanchez Escribano, G. Busca, Appl. Catal. A Gen. 166, 75 (1998)
- [2] A.V. Olmos, R. Redon, G.R. Gattorno, M.E.M. Zamora, F.M. Leal, A.L.F. Osorio, J.M. Saniger, J. Colloid Sci. 291, 175 (2005)
- [3] W.M. Wang, Y.N. Yang, J.Y. Zhang, Appl. Catal. A 133, 81 (1995)
- [4] M. Baldi, E. Finonnhio, F. Milella, G. Busca, Appl. Catal. B: Environ. 16, 43 (1998)
- [5] M.C. Bernard, H.L. Goff, B.V. Thi, J. Electrochem. Soc. 140, 3065 (1993)
- [6] Y. Yamashita, K. Mukai, J. Yoshinobu, M. Lippmaa, T. Kinoshita, M. Kawasaki, Surf. Sci. 514, 54 (2002)
- [7] V. Berbenni, A. Marini, J. Anal. Appl. Pyrolysis 70, 437 (2003)
- [8] L. Sanchez, J. Farcy, J. Tirado, J. Mater. Chem. 6, 37 (1996)
- [9] W. Wang, C. Xu, G. Wang, Y. Liu, C. Zheng, Adv. Mater. 14, 837 (2002)
- [10] W. Zhang, Z. Yang, Y. Liu, S. Tang, X. Han, M. Chen, J. Cryst. Growth 263, 394 (2004)
- [11] Z. Weixin, W. Cheng, Z. Xiaoming, X. Yi, Q. Yitai, Solid State Ion. 117, 331 (1999)
- [12] J.C. Southard, G.E. Moore, J. Am. Chem. Soc. 64, 1769 (1942)
- [13] E. Finocchio, G. Busca, Catal. Today 70, 213 (2001)
- [14] Y.C. Zhang, T. Qiao, X.Y. Hu, J. Solid State Chem. 177, 4093 (2004)
- [15] G. Demazeau, J. Mater. Chem. 9, 15 (1999)
- [16] Y.Q. Chang, X.Y. Xu, X.H. Luo, C.P. Chen, D.P. Yu, J. Cryst. Growth 264, 32 (2004)

- [17] S.K. Apte, S.D. Naik, R.S. Sonawane, B.B. Kale, N. Pavaskar, A.B. Mandale, B.K. Das, Mater. Res. Bull. 41, 647 (2006)
- [18] M. Anilkumar, V. Ravi, Mater. Res. Bull. 40, 605 (2005)
- [19] A. Baykal, Y. Köseog `lu, M. Senel, Central Eur. J. Chem. 5, 169 (2007)
- [20] O.Yu. Gorbenko, I.E. Graboy, V.A. Amelichev, A.A. Bosak, A.R. Kaul, B. Guttler, V.L. Svetchnikov, H.W. Zandbergen, Solid State Commun. 124, 15 (2002)
- [21] A. Askarinejad, A. Morsali, Ultrason Sonochem 16, 124 (2009)
- [22] Z.W. Chen, J.K.L. Lai, C.H. Shek, Scr. Mater. 55, 735 (2006)
- [23] T. Ozkaya, A. Baykal, H. Kavas, Physica B-Condensed Matter. 403, 19 (2008)
- [24] Z. Weixin, W. Cheng, Z. Xiaoming, X. Yi, Q. Yitai, Solid State Ionics 117, 331 (1999)
- [25] J.M. Boyero, E.L. Fernández, J.M. Gallardo-Amores, R.C. Ruano, V.E. Sánchez, E.B. Pérez, Int. J. Inorg. Mater. 3, 889 (2001)
- [26] F.A. Al Sagheer, M.A. Hasan, L. Pasupulety, M.I. Kaki, J. Mater. Sci. Lett. 18, 209 (1999)
- [27] B. Gillot, M. El.Guendouzi, M. Laarj, Materials Chemistry and Physics 70, 1 (2001)
- [28] S. Brunauer, L. Deming, W. Deming, E. Teller, J. Am. Chem. Soc. 62, 7 (1940)
- [29] K.S.W. Sing, D.H. Everett, R.A.W. Haul, Pure & Appl. Chem. 57, 4 (1985)
- [30] J. Rouquerol, D. Avnir, C.W. Fairbridge, Pure & Appl. Chem. 66, 8 (1994)